PROCEEDINGS OF SCIENCE

arXiv:1602.05965v1 [astro-ph.HE] 18 Feb 2016

Modeling *Fermi* Large Area Telescope and Multiwavelength Data from Blazars

Justin D. Finke*
U.S. Naval Research Laboratory, Code 7653, 4555 Overlook Ave. SW, Washington, DC 20375 USA
E-mail: justin.finke@nrl.navy.mil

Blazars are active galactic nuclei with relativistic jets pointed at the Earth, making them extremely bright at essentially all wavelengths, from radio to gamma rays. I will review the modeling of this broadband spectral energy distributions of these objects, and what we have learned, with a focus on gamma rays.

3rd Annual Conference on High Energy Astrophysics in Southern Africa -HEASA2015, 18-20 June 2015
University of Johannesburg, Auckland Park, South Africa

*Speaker.

This is a United States government work published under licence.

1. Introduction

In this proceeding, I review results of multi-wavelength modeling of *Fermi* LAT-detected blazars. It is an update of my previous short review from the *Fourth Fermi Symposium* [62]. The remainder of this section is devoted to a basic introduction to blazars. In Section 2 I discuss some results of population studies of blazars, with an emphasis on the blazar sequence. Section 3 is devoted to a discussion of the origin of the curvature in the γ-ray spectra of some blazars, one of the major discoveries of the *Fermi*-LAT that does not currently have a good explanation. Another major open problem in blazar physics is the question of where in the jet the γ-ray flares are produced, and this is the topic of Section 4. One of the defining characteristics of blazars is that they are highly variable, and so this is discussed in Section 5. Finally, in Section 6, a brief description of hadronic models for γ-ray emission in blazars is given.

1.1 The *Fermi Gamma Ray Space Telescope*

The *Fermi Gamma Ray Space Telescope*, launched from Cape Canaveral, Florida, USA, on 2008 June 11 has two instruments, the Large Area Telescope (LAT), and the Gamma-Ray Burst Monitor. Only the former will be discussed here. The LAT is a pair conversion telescope sensitive to photons in the 20 MeV to 300 GeV range with about 0.8° resolution for a single photon [23]. It sees about 20% of the sky at any one time, and surveys the entire sky every 3 hours. Eighty-five percent of the 2023 associated or identified sources in the most recent *Fermi* LAT Catalog, the 3FGL, are *blazars* [11].

1.2 Blazars and Their Basic Properties

It is thought that almost all (if not all) galaxies have supermassive black holes ($M_{BH} \sim 10^6 - 10^{10}\ M_\odot$) at their centers. About 20% of these have bright nuclei powered by accretion onto the supermassive black hole, and are known as active galactic nuclei (AGN; [85]). About 15-20% of these are radio loud [86], with their radio emission being due to a relativistic jet. Quasars with flat radio spectra are thought to have their jet pointed towards the Earth. The flat spectrum radio quasars and BL Lacertae objects together are known as blazars. They are characterized by multi-wavelength highly variable (timescales as short as minutes in some cases) nonthermal emission at essentially all frequencies, from radio to γ-rays. They are thought to be misaligned radio galaxies, which have extended jets not pointed towards our line of sight, terminating in radio lobes at $\sim$0.1–1 Mpc distances from the black hole.

Individual components in blazar jets have been resolved with radio very long baseline interferometry (VLBI). There is considerable evidence that these individual components are traveling at a large fraction β of the speed of light c (giving them a bulk Lorentz factors $\Gamma = (1-\beta)^{-1/2}$) at small angles ($\theta$) to our line of sight. This evidence includes:

- Extremely high radio surface brightnesses, which would require extreme energy densities if produced by synchrotron from stationary sources (e.g.,[80, 81]).

- On the milliarcsecond scale, jet components can be resolved with radio VLBI (e.g. [93]) and they often appear to have apparent speeds $v_{app} = \beta_{app} c > c$, which can be explained by

blobs moving at near the speed of light ($\beta \sim 1$, $\Gamma \gg 1$) with angles close to the line of sight ($\theta \ll 1$). In this case their apparent speed is[1]

$$\beta_{app} = \frac{\beta \sin\theta}{1-\beta\cos\theta} = \delta\Gamma\beta\sin\theta \approx 10\ \delta_1^2(\Gamma/\delta)\theta_{-1} \tag{1.1}$$

where $\delta = [\Gamma(1-\beta\cos\theta)]^{-1}$.

- The detection of rapid γ-ray flares from blazars implies the blob must be moving with $\Gamma \gg 1$ in order for the γ rays to escape and avoid $\gamma\gamma$ attenuation (e.g., [53]).

This geometry leads to a number of observational consequences. Events in the blob will appear in "fast forward", so that the observer sees a time interval $t = (1+z)t'/\delta$ where t' is some time interval in the frame comoving with the blob[2] and z is the cosmological redshift. Light-travel time effects imply that a spherical blob must have a radius

$$R'_b \leq \frac{\delta c t_v}{1+z} = 3\times 10^{15}\ \delta_1 t_{v,4}(1+z)^{-1}\ \text{cm} \tag{1.2}$$

where t_v is the variability time, approximately the time it takes the flux to change by a factor of 2. The observed photon energy is "blueshifted" $\varepsilon = \delta\varepsilon'/(1+z)$, and the flux is "Doppler-boosting" so that if the comoving frame νF_ν synchrotron flux is f'_{sy}, the observer sees $f_{sy} = \delta^4 f'_{sy}$. A blob with $\delta = 10$ appears $\sim 10^4$ times brighter than it would if it was stationary.

1.3 Blazar Spectral Energy Distributions (SEDs)

Blazars' spectral energy distributions (SEDs) have two components (Figure 1): a low-frequency component, peaking in the infrared to X-rays, almost certainly from synchrotron emission; and a high-frequency component, peaking at γ-ray energies. The origin of the γ-ray component is not completely certain, but it is probably due to the Compton-scattering of a seed photon source which could be either the synchrotron photons themselves, in which case it is known as synchrotron self-Compton (SSC); or they could be external to the jet, often known as external Compton (EC). The source of seed photons for EC could be the accretion disk [48, 49], broad-line region (BLR; [130]), dust torus [84], or even other components of the jet [71, 94]. The broadband emission is usually modeled as being from a single component (a "one zone" model") where all the emission is generated by a single population of electrons, except for the radio which is thought to be from the superposition of several self-absorbed components [87]. This can be justified to some extent by correlated variability between several wavebands (e.g., [67, 17, 29, 38, 124, 44]).

Aside from Compton scattering, γ rays could also be produced by protons co-accelerated in the jet with the electrons. This is motivated by the fact that blazars are a leading contender to be the origin of ultra-high energy cosmic rays (UHECRs; e.g., [47]). Protons could produce γ rays directly through synchrotron emission or through the synchrotron emission of child particles produced through pγ interactions [96, 95, 107, 108].

[1] I will use the notation $A_x = 10^x A$ with Gaussian/cgs units unless otherwise stated.

[2] In general, primed quantities will refer to this comoving frame and unprimed quantities will refer to the observer frame.

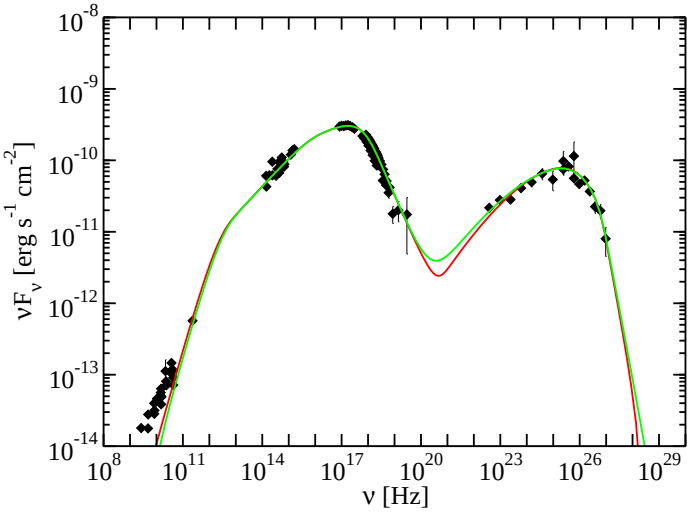

Figure 1: The SED of the HSP BL Lac object Mrk 421, with $\nu_{pk}^{sy} \approx 10^{17.3}$ Hz. Figure taken from [8].

1.4 Classification of Blazars

Blazars are classified in two basic ways: based on their emission line properties, and based on the peak frequency of their synchrotron component.

The classification of blazars based on their emission lines has changed several times, but basically, blazars are classified as *BL Lac objects* if the equivalent width of their broad lines are less than a certain value, and as *Flat Spectrum Radio Quasars (FSRQs)* otherwise, taking into account the strength of the Ca H & K break [133, 97] and possibly narrow emission lines [91]. A different, more physical transition based on luminosity was suggested by Ghisellini et al. [73]. They proposed that those with broad line luminosity as a fraction of Eddington $L_{BLR}/L_{Edd} < 5 \times 10^{-4}$ be considered BL Lac objects, while those with $L_{BLR}/L_{Edd} > 5 \times 10^{-4}$ be considered FSRQs. BL Lacs are thought to be associated with Fanaroff-Riley (FR; [61]) type I radio galaxies, and FSRQs with FR type II radio galaxies [138], although exceptions are known to exist (e.g., [90]).

Blazars are also classified based on the frequency of their synchrotron peak, ν_{pk}^{sy}. In the latest incarnation of this, they are considered low-synchrotron peaked (LSP) if $\nu_{pk}^{sy} < 10^{14}$ Hz; intermediate-synchrotron peaked (ISP) if 10^{14} Hz $< \nu_{pk}^{sy} < 10^{15}$ Hz; and high-synchrotron peaked if $10^{15} < \nu_{pk}^{sy}$ Hz [6]. Almost all FSRQs are LSPs [13, 14]. Blazars are highly variable, and their peak frequency can change over time (e.g., [72]). This means that the classification of a blazar can depend on the epoch it was observed.

2. Population Studies

2.1 Blazar Sequence

A useful tool in stellar astrophysics is the Hertzsprung-Russell diagram, which describes the luminosity and the optical spectral type (related to temperature and color) of stars and includes the very prominent main sequence, on which stars spend a large fraction of their lifetimes. Due to its

success in understanding stars, it is tempting to look for a similar diagram for blazars. A "blazar main sequence" or "blazar sequence" was suggested by Fossati et al. [68], combining three samples of blazars ([88, 140, 57]). They found three parameters that appeared to be well-correlated with ν_{pk}^{sy}: the 5 GHz radio luminosity, the luminosity at the peak of the synchrotron component (L_{pk}^{sy}), and the "γ-ray dominance", i.e., the ratio of of the γ-ray luminosity (L_γ; as measured by EGRET) and the peak luminosity of the synchrotron component (L_{pk}^{sy}). The existence of these correlations in subsequent studies is a matter of some debate [118, 115, 40, 63].

Nevertheless, Ghisellini et al. [70] suggested a physical explanation for these correlations. For nonthermal electrons accelerated as power-laws and allowed to escape a region of size R' and cool through synchrotron and Compton losses, a "cooling break" is found in the electron distribution at electron Lorentz factor given by

$$\gamma_c' = \frac{3m_e c^2}{4c\sigma_{\rm T} u_{tot}' t_{esc}'} \, , \tag{2.1}$$

where $m_e = 9.1 \times 10^{28}$ g is the electron mass, $\sigma_{\rm T} = 6.65 \times 10^{-25}$ cm is the Thomson cross section, $t_{esc}' \cong R'/c$ is the escape timescale, and u_{tot}' is the total energy density in the frame of the relativistic blob, given by the sum of the Poynting flux (u_B'), synchrotron (u_{sy}'), and external radiation field ($u_{ext}' \cong \Gamma^2 u_{ext}$) energy densities. The cooling Lorentz factor γ_c' is associated with a peak in the synchrotron spectrum of the source in a νF_ν representation observed at frequency

$$\nu_{pk}^{sy} = 3.7 \times 10^6 \, \gamma_c'^2 \, \left(\frac{B}{\rm G}\right) \, \frac{\delta}{1+z} \, {\rm Hz} \tag{2.2}$$

(e.g., [135]) where B is the magnetic field in the blob. For objects that have weak external radiation fields so that $u_B' \gg u_{ext}'$, and neglecting u_{sy}', Equations (2.1) and (2.2) give

$$\nu_{pk}^{sy} \cong 2.2 \times 10^{15} \, B_0^{-3} \, \delta_1 \, (1+z)^{-1} \, \, R_{15.5}'^{-2} \, {\rm Hz} \, . \tag{2.3}$$

These objects are HSPs. Objects with a strong external radiation fields from the broad line region (BLR) which dominate over u_B' and u_{sy}', have peak synchrotron frequencies given by

$$\nu_{pk}^{sy} \cong 3.2 \times 10^{12} \, \, B_0 \, \delta_1^{-3} \, (\delta/\Gamma)^4 \, (1+z)^{-1} \, \, R_{15.5}'^{-2} \, u_{ext,-2}^{-2} \, {\rm Hz} \, . \tag{2.4}$$

These objects are LSPs. Thus far, all HSP blazars ($\nu_{pk}^{sy} > 10^{15}$ Hz) discovered have been BL Lac objects with weak if any broad emission lines, while almost all FSRQs, with strong emission lines, have been LSPs ($\nu_{pk}^{sy} < 10^{14}$ Hz). However, there are a significant number of BL Lacs which are LSPs. Objects with stronger line emission would also be expected to have greater γ-ray dominances, due to scattering of the external radiation field. Ghisellini et al. [70] thus predicted a sequence of blazars, from low power, high peaked, low γ-ray dominance, lineless objects, and as the external radiation field increases, to low peaked, high γ-ray dominance objects with strong broad emission lines.

In all of the *Fermi*-LAT AGN catalogs, a correlation between γ-ray spectral index (Γ_γ) and ν_{pk}^{sy} has been found [1, 6, 5, 13, 14]. This correlation was explained by Dermer et al. [50]. As the synchrotron peak moves to higher frequencies, Compton peak will also move to higher frequencies, resulting in harder γ-ray spectra, for a jet blob with a log-parabola electron distribution that is in near-equipartition with the Poynting flux. This could also represent a diagram around which one could build a "blazar main sequence".

2.2 Alternative Explanations for the Blazar Sequence

An alternative explanation for the correlations found by Fossati et al. was given by Giommi and collaborators [75, 77, 76]. They propose that the sequence is a result of a selection effect: luminous blazars with high synchrotron peaks have their spectral lines totally swamped by the nonthermal continuum, making a redshift measurement impossible. Without a redshift, it is not possible to determine their luminosities, and so they are not included in statistical tests that measure a correlation between luminosity and ν_{pk}^{sy}. There is some evidence for this [125, 117], although see Meyer et al. [104] and Ghisellini et al. [74]. However, an intrinsic quantity that can be determined without redshift could be used in place of luminosity. The blazar sequence as originally found by Fossati et al. [68] included the γ-ray dominance. Note also that ν_{pk}^{sy} is only weakly dependent on redshift, by a factor $(1+z)$, i.e., a factor of a few. The *Fermi*-LAT allows the γ-ray dominance and the Compton dominance ($A_C \equiv L_{pk}^{C}/L_{pk}^{sy}$ where L_{pk}^{C} is the luminosity at the Compton peak) to be found for more blazars than in the EGRET era. A plot of A_C versus ν_{pk}^{sy} is shown in Fig. 2, from a subset of sources in the second LAT AGN catalog [13], including sources that do not have known redshifts. A correlation clearly exists, as shown by the Spearman and Kendall tests [63], so that this aspect of the blazar sequence does seem to have a physical origin.

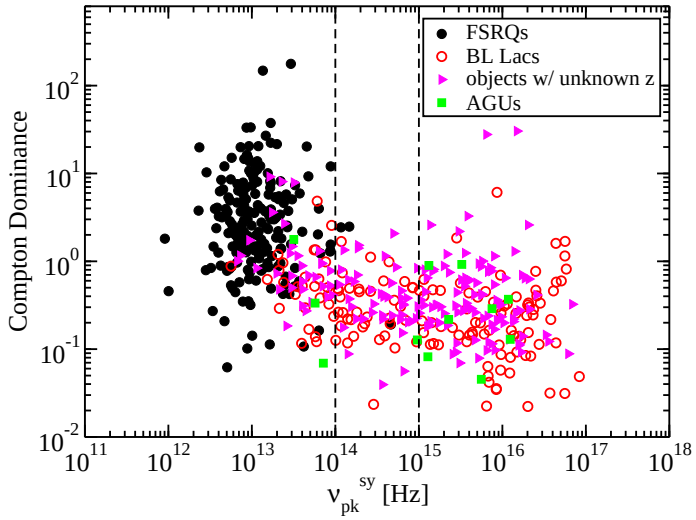

Figure 2: Compton dominance (i.e., L_{pk}^{C}/L_{pk}^{sy}) versus peak synchrotron frequency. Filled circles represent FSRQs, empty circles represent BL Lacs, and filled squares represent objects which do not have an unambiguous classification. Rightward-pointing triangles represent BL Lacs with unknown redshifts, for which ν_{pk}^{sy} is a lower limit. Figure taken from [63].

Meyer et al. [103] proposed another physical scenario, based on updated data from a number of sources. In their scenario, the difference between BL Lacs and FSRQs is the former have jet structure with velocity (or Lorentz factor) gradients, either perpendicular or parallel to the direction of motion, while FSRQs do not have these gradients. They have a single Lorentz factor for the entire jet, or at least the radiatively important parts. There is indeed evidence for different Lorentz factors in BL Lacs and FRIs (e.g., [43, 42, 3]). The lack of γ-ray detected FRIIs hints that FRIIs/FSRQs do

not share this jet structure [78], although, see [31] for evidence of jet deceleration in an FSRQ. The scenario of [103] predicts that there should be no radio galaxies with $\nu_{pk}^{sy} \gtrsim 10^{15}$ Hz, since these will be only the most aligned BL Lac sources. However, radio galaxies have recently been found with peaks this high [69], so that the scenario of Meyer et al. may need revision.

2.3 Blazar Evolution

The LAT γ-ray luminosity functions, luminosity densities, and number densities, and their evolution with redshift have been explored by M. Ajello and collaborators [19, 18]. As one goes to higher redshift, the number density of FSRQs increases up to $z \approx 0.5$, where it begins to decrease. By contrast, the number density of HSP BL Lacs always decreases as one goes to higher z, with significantly steeper decrease between $z \approx 0.0 - 0.5$. Ajello et al. suggested that this may be due to FSRQs turning into BL Lac objects at redshifts $z \lesssim 0.5$. This provides some evidence for an evolutionary scenario for the blazar sequence, as outlined by Böttcher & Dermer [30] and Cavaliere & D'Elia [35]. In this scenario, FSRQs are younger objects and have substantial circum-nuclear material making up the accretion disk and broad-line region (BLR), which is slowly accreted onto the black hole. As the circum-nuclear material accretes, the broad emission lines decrease, and the accretion rate decreases, and the sources become older BL Lac objects.

3. Gamma-Ray Spectral Curvature

After the launch of *Fermi*, while the spacecraft was still in its post-launch commissioning and checkout phase, the FSRQ 3C 454.3 was detected by the LAT in an extreme bright state [137]. The source reached a flux of $F(>100\ \mathrm{MeV}) > 10^{-5}$ ph cm^{-2} s^{-1} and its spectrum showed an obvious curvature (i.e., a deviation from a single power-law), which was best-fit by a broken power-law [2] with break energy ~ 2 GeV. This source flared on several more occasions [15, 7], exhibiting a spectral break (or spectral curvature) during bright states. The energy of the break varied by no more than a factor of ~ 3, while the flux varied by as much as a factor of 10 [7]. This spectral curvature has been found in other blazars as well, although a broken power-law is not always preferred over a log-parabola fit, which has one less free parameter [4]. The spectral break (curvature) is not always present in flaring states of 3C 454.3 and other blazars [116]. The cause of the curvature is not clear but there are several possible explanations, which are briefly reviewed below.

3.1 Combination of Several Scattering Components

It was noted that, based on the shape of the optical and γ-ray spectra, the Compton scattering of more than one seed photon source was needed to explain the overall spectral energy distribution (SED) of 3C 454.3 [66]. The particularly soft spectra above the break requires that this scattering be done in the Klein-Nishina (KN) regime. The FSRQ PKS 1424$-$418 had an unusual (although not statistically significant) "upturn" in its LAT spectrum that was modeled as the combination of several scattering components by Buson et al. [34]. In order for this scenario to be viable, the γ-ray emitting region must be within the BLR.

3.2 Compton Scattering of BLR Lyα Photons

For the scattering of Lyα photons ($E_* = 10.2$ eV), the KN regime will emerge at energies above

$$E_{KN} \approx 1.2\ (E_*/10.2\ \mathrm{eV})^{-1}\ \mathrm{GeV}\ , \tag{3.1}$$

approximately in agreement with the observed break energy [15]. Fits with this model using power-law electron distributions failed to reproduce the observed LAT spectra [15]; however, fits using a log-parabola electron distribution were able to reproduce the γ-rays [36]. This model would also require the γ-ray emitting region to be within the BLR.

3.3 Curvature in the electron distribution

Abdo et al. [2] suggested that if there is curvature in the electron distribution that produces the γ-rays, presumably from Compton scattering, this would naturally be reflected in the LAT spectrum as well. In this scenario, one would expect the curvature in the electron distribution to cause a curvature in the synchrotron emission from the same electrons, which would appear in the IR/optical. Indeed, observations of PKS 0537−441 do show this curvature (see Fig. 3; [45]). This explanation would not require scattering to take place in the BLR, as dust torus photons could be the seed photon source for scattering.

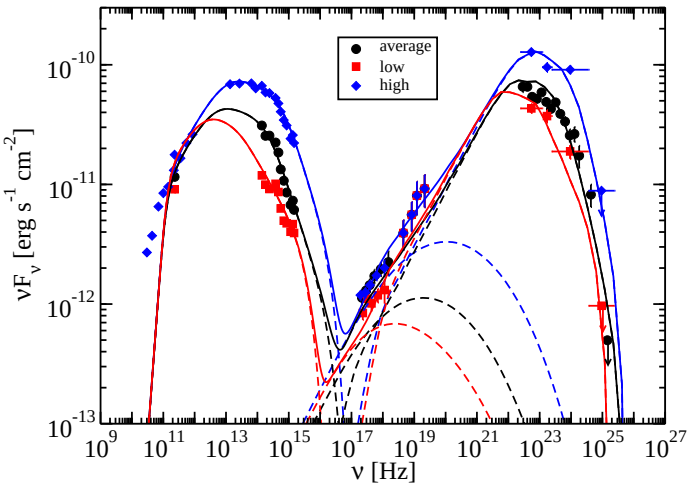

Figure 3: SED of the FSRQ PKS 0537−441 [45]. The spectral curvature in the IR/optical in the high state could indicate the cause of the γ-ray curvature is the result of curvature in the electron distribution.

3.4 Photoabsorption in the Broad Line Region

Poutanen & Stern [122] modeled the breaks at a few GeV with $\gamma\gamma$ absorption features from interactions of the γ rays with He II Lyα and recombination photons (54.4 eV and 40.8 eV, respectively) from the BLR. The existence of these breaks was disputed by Harris et al. [79]. A few years later, with an updated analysis including more LAT data (almost 5 years) and updated instrument

response functions, Stern & Poutanen [132] found instead that the absorption features were at ~ 10 GeV, with they interpreted as being from $\gamma\gamma$ absorption by H Lyman continuum photons (13.6 eV). An absorption feature at this energy was actually predicted before the launch of *Fermi* by Reimer [126]. The $\gamma\gamma$ absorption optical depths implied by the fits to the LAT data by Stern & Poutanen [132] were quite a bit lower than expected, $\tau_{\gamma\gamma} \sim 2-5$, compared to $\tau_{\gamma\gamma} \approx 100$ that one would expect if the γ rays were produced deep inside the BLR. They proposed several possible explanations for this: the size of the Lyman continuum BLR is larger than expected; a flattened geometry for the BLR, leading to much of the BLR photons being at an unfavorable geometry for $\gamma\gamma$ absorption; and finally, there may be several places along the jet where γ rays are emitted, some inside and some outside the BLR, and all of these flares contribute to the γ-ray spectrum integrated over several years. The γ rays from inside could be "diluted" by photons from outside, creating the illusion of less absorption.

3.5 Conversion to Axion-Like Particles

Axion-like particles (ALPs) have been proposed in several predictions of standard model extensions (e.g., [127]). It may be possible for photons to transform into ALPs and back again in the presence of a magnetic field. It has been shown that this could fit the spectral curvature seen in the γ-ray spectrum of 3C 454.3 [102], as well as allow photons to escape the BLR that otherwise might not be able to do so [136, 102].

4. Location of Gamma-Ray Emitting Region

In recent years, there has been an intense debate as to the location of the γ-ray emitting region in FSRQs, with no consensus yet reached. There are two main options: inside the BLR, within ~ 0.1 pc from the black hole, where BLR photons are the likely seed photon source for Compton scattering, and $\gtrsim 1$ pc, where the dust torus is the likely source of seed photons. These possibilities are explored below, with some ways to distinguish them based on γ-ray light curves and gravitational lensing.

4.1 Gamma Rays Produced Inside the BLR

Rapid variability in FSRQs such as 3C 454.3 ($t_v \sim 3$ hours; [134]), and PKS 1510$-$089 ($t_v \sim 1$ hour; [33, 129]) limits the size of the emitting region by Equation (1.2). If the emitting region takes up the entire cross section of a conical jet with half-opening angle α, then it should be at a distance

$$r \leq 0.1\ \delta_1\ t_{v,4}\ \alpha_{-2}^{-1}\ (1+z)^{-1}\ \text{pc} \tag{4.1}$$

from the base of the jet. Based on scaling relations found from reverberation mapping, the typical BLR region for FSRQs is $r_{BLR} \sim 0.1$ pc $\approx 10^{17}$ cm (e.g., [28, 27]), so that the emitting region would likely be within the BLR. An emitting blob inside the BLR would move outside of a BLR with radius R_{BLR} in a time period (assuming $\theta \ll 1$)

$$\Delta t = 3.3 \times 10^4\ R_{BLR,17}\ \delta_1^{-2}\ (\delta/\Gamma)\ (1+z)\ \text{s} \tag{4.2}$$

in the observer's frame. So if a γ-ray flare is found to last longer than 9 hours or so, it must have moved out of the BLR, or be made up of many smaller flares from several different blobs.

The cooling timescale in the observer's frame for electrons producing photons observed at $E_{obs} = 1$ GeV, assuming a high Compton dominance and scattering of Lyman α BLR photons ($E_0/(m_e c^2) = 2 \times 10^{-5}$) , is

$$t_{cool} = 4400\ u_{ext,-2}^{-1}\ \delta_1^{-2}\ (\delta/\Gamma)^2\ E_{0,Ly\alpha}^{1/2}\ E_{\rm obs,GeV}^{-1/2}\ (1+z)^{1/2}\ {\rm s} \tag{4.3}$$

which implies the electrons can completely cool before the blob moves out of the BLR.

4.2 Gamma Rays Produced Outside the BLR

Optical and γ-ray flares in FSRQs are often associated with a slow increase in radio flux which peaks after the γ-ray flare [89, 92], and the ejection of superluminal components from the 43 GHz core (e.g., [83, 99, 100]). According to Marscher [101], 2/3 of γ-ray flares are associated with the ejection of a superluminal component, from which the conclusion is drawn that the γ-ray flares are coincident with the 43 GHz core, located at a few pc from the black hole, outside the BLR (e.g., [100, 123]). There are two arguments that the 43 GHz core, and thus the γ-ray flares occur, at $r > 1$ pc from the black hole, outside the BLR.

1. The 43 GHz core has observed radius R_{core} and the jet has known half-opening angle α from VLBI observations (e.g.,[82]). This gives the distance of the core from the black hole, $r = R_{core}/\alpha$, which for AO 0235+164, gives a distance of $r \gtrsim 12$ pc [16].

2. The time scales for the radio outbursts are $\Delta t \sim$ 10s of days. During this time blobs will have had to travel distances

$$r \approx 1.0\ \Delta t_6\ \delta_1^2\ (\Gamma/\delta)\ (1+z)^{-1}\ {\rm pc} \tag{4.4}$$

   before the γ-ray flares and ejections of the superluminal components. Nalewajko et al. [111] found a possible way to explain the delay with a light-travel time effect that could allow γ-ray flares to occur at much smaller distances than the location of the 43 GHz core.

Additionally, γ-ray flares with emission up to 100s of GeV have been detected with imaging atmospheric Cherenkov telescopes from several FSRQs, including 3C279 [20], PKS 1510−089 [10, 21], 4C 21.35 [22, 12], B0218+357 [105], and PKS 1441+25 [106, 109]. If these flares occurred inside the BLR, they would suffer extreme $\gamma\gamma$ absorption (see Section 3.4), and these γ rays would not have been observed. Flares detected out to several 10s of GeV by the LAT [116] are also not likely to originate from inside the BLR for the same reason. Several ways have been suggested to avoid $\gamma\gamma$ attenuation, such as through transport by neutron beams [46] or axions [136]. If rapid variability ($t_v \sim 10^4$ s) does occur at $\gtrsim$ pc scale distances from the black hole, it would mean the emitting region makes up a small fraction of the jet cross section, which might be a problem for a standard "shock in jet" model.

Outside the BLR, a likely source of seed photons is the dust torus. The region where scattering of dust photons is geometrically likely is $r < R_{dust}$ where

$$R_{dust} = 1.1\ L_{disk,45}^{1/2}\ T_3^{-2.6}\ {\rm pc} \tag{4.5}$$

is the inner radius of the dust torus (the sublimation radius), L_{disk} is the disk temperature, and T is the temperature at dust here [112, 113]. This constrains the energy density from the dust torus to be

$$u_{dust} = 2.3 \times 10^{-5}\ \xi_{-1} T_3^{5.2}\ {\rm erg\ cm^{-3}} \tag{4.6}$$

where $\xi \leq 1$ is the fraction of the disk emission reprocessed by the dust torus. An emitting blob with $r < R_{dust}$ moves outside in a time period

$$\Delta t = 13\ \delta_1^{-2}\ (\delta/\Gamma)\ L_{disk,45}^{1/2}\ T_3^{-2.6}\ (1+z)\ \text{day}\ . \tag{4.7}$$

The cooling timescale for the electrons making LAT-energy γ rays by scattering dust torus photons is

$$t_{cool} = 3.5\ \xi_{-1}^{-1}\ T_3^{-4.7} \delta_1^{-2}\ (\delta/\Gamma)^2\ E_{\rm obs,GeV}^{-1/2} (1+z)^{1/2}\ \text{day}\ . \tag{4.8}$$

Thus the electrons will have enough time to cool before leaving the dust torus. Note that the energy density and cooling timescale are strongly dependent on the dust temperature, which cannot exceed $T_3 \approx 2$ or else it will sublimate. The dust torus can only act as the seed photon source if $r < R_{dust} \sim 1$ pc. However, as described above, there is evidence that it can exceed this distance, in which case another seed photon source is needed. Another possibility is the scattering of photons from other parts of the jet [71, 98, 94]. Zacharias & Schlickeiser [141] fit several FSRQs with a synchrotron/SSC model without an EC component, offering another possibility.

4.3 Gamma Ray Light Curves

One possible way to determine the seed photon source for EC has been suggested by Dotson et al. [55]. This would effectively resolve the question of the location of the γ-ray emitting region (Section 4), since if the region is withing the BLR, the seed photons will be at a much higher energy (≈ 10 eV for Lyα) than if they are from a ≈ 1000 K blackbody. This involves exploiting the Klein-Nishina cross section. Due to the turnover in the Compton-scattering cross section at high energies, the relative cooling of electrons producing γ rays at different energies will be different for different seed photon energies, which could be used to constrain the seed photon energy. This requires using at least two LAT light curves with two different energy ranges. The approximate timescales of the flares needed can be found from Equations (4.3) and (4.8). Application of this technique to several bright flares from PKS 1510$-$089 observed in 2009 indicates that some flares are produced inside the BLR, while some are produced outside [54].

4.4 Gravitational Lensing

Gravitational lensing of a blazar by an intervening galaxy can produce multiple images of the blazar. The images will have different brightnesses and the light curve of one will be delayed with respect to the other. Although the images can often be resolved with radio telescopes, this is not possible with the larger PSF of γ-ray telescopes. However, the differing brightness and time delay allow for the possibility that one can distinguish the γ-ray light curves of two lensed images, particularly during bright flares. Barnacka et al. [26] claimed the first detection of a gravitationally lensed time delay in γ-rays in the LAT light curve of the FSRQ PKS 1830$-$211 (although see [9]) and another γ-ray gravitational lens-induced delay was found from the blazar B0218+357 [41]. For some of the bright γ-ray flares reported in the literature thus far, either the magnification ratio (the ratio of the brightness of two lensed images), or the time delay, or both, are not consistent with the ones measured from the radio images. This has been interpreted in two ways.

One interpretation is that the location of the emitting region is different for γ-ray flares than most of the radio emission [24]. In this case, carefully modeling the lens system can constrain the

location of the γ-ray emitting region in the jet. For two γ-ray flares detected from PKS 1830−211, the location of the flares were constrained to originate at $\gtrsim 1$ kpc projected distance from the radio core, or $\gtrsim 10$ kpc deprojecting with a jet angle to the line of sight of $\theta = 0.1$ rad [25]. This is far beyond the BLR and dust torus, so that it is not clear what the seed photon source would be for EC at these large distances.

Another possible interpretation is microlensing by individual stars in the lensing galaxy. If this is the case, the size of the γ-ray emitting region can be constrained. This has been used to constrain it to be $R \sim 10^{14}$ cm for flares in both PKS 1830−211 [114] and B0218+357 [139]. Assuming the emitting region takes up this entire cross section of the jet (see Section 4.1), this constrains its location to be $r \sim 10^{16}\ \alpha_{-2}^{-1}$ cm from the base of the jet. The blazar B0218+357 has been detected at > 100 GeV by MAGIC [105]. It is not clear if this source has a significant BLR, and it is classified as a "blazar of uncertain type" in BZCAT[3], but if it does, it is not clear how γ-ray photons would escape avoiding $\gamma\gamma$ absorption with BLR photons (see Section 4.2).

5. Variability

One of the defining characteristics of blazars is extreme variability across the electromagnetic spectrum, on timescales as short as minutes in some cases. Here I briefly describe a few results from modeling blazar variability.

5.1 SEDs at Different Epochs

A number of FSRQs have been modeled with time-independent synchrotron/SSC/EC models in several states, and an interesting pattern is emerging. For many sources, the quiescent and flaring states can be modeled by changing only the electron distribution between states–that is, the other parameters, magnetic field, Doppler factor, etc., are not changed. This includes flares from PKS 0537−441 [45] (see Figure 3), PKS 1830−211 [9], and 4C 21.35 [12]. For other sources, different flares can be modeled by changing at least one additional parameter (usually the magnetic field), while for other flares from the same sources, only changes in the electron distribution are needed. These include PKS 2142−75 [56] and PKS 1424−418 [34]. Flares where another parameter is needed are usually those where γ-ray flares occur without corresponding optical flares, or optical flares without corresponding γ-ray flares [39, 44].

5.2 Multi-Wavelength Light Curves

Recently, several authors have begun modeling the multi-wavelength light curves of blazars with time-dependent leptonic models. Saito et al. [128] have modeled a bright LAT-detected γ-ray flare from PKS 1510−089 with duration $\sim$ a few hours in 2011 November. Unfortunately, light curves at other wavelengths are not available for this flare. Using a model of a shock traveling through a helical magnetic field, Zhang et al. [144] were able to reproduce the light curves, including polarization angle and degree as a function of time, for a flare from 3C 279 with duration ~ 20 days.

[3] http://www.asdc.asi.it/bzcat/

5.3 Fourier Analysis

Theoretical work has also been done on reproducing the power spectral densities of blazars. A one-zone model was created where variability is caused by only variability in the electron injection rate, assumed to be injected stochastically as as a power-law in Fourier frequency (i.e., red noise) with index a. The model predicts that at low frequencies, synchrotron and EC PSDs would be $S(f) \propto f^{-a}$, while SSC PSDs would be $S(f) \propto f^{-(2a-2)}$ [64]. This predicts a separation in the index in the LAT PSDs of BL Lacs and FSRQs, assuming BL Lacs emit γ rays by SSC and FSRQs emit γ rays by EC. The predicted separation was in fact seen in the LAT PSDs calculated by Nakagawa & Mori [110], however, not in the LAT PSDs calculated by Sobolewska et al. [131] or Ramakrishnan et al. [123].

At higher frequencies, for synchrotron and EC, one expects breaks in the PSDs of blazars, so that the power-law index will change from a to $a+2$. The frequency of the breaks will be related to the cooling timescale. Finding this break in the γ-ray PSDs at several LAT energies could be used to constrain the seed photon energy [65], similar to the method described by Dotson et al. [55] (see Section 4.3).

6. Hadronic Models

In the *Fermi* era, several authors have fit the SEDs of LAT-detected blazars with hadronic models. Here we briefly review a few of the results from hadronic modeling.

Böttcher et al. [32] have modeled the SEDs of a dozen blazars, all of which are LSP or ISP type and half of which are FSRQs, with the synchrotron proton blazar model [107, 108]. In many cases the models implied jet powers of $P_j \sim 100 - 1000 L_{Edd}$, which seems to strongly disfavor these models [142]. This is consistent with the result of Petropoulou & Dimitrakoudis [119], who find that the synchrotron proton model is disfavored for the FSRQ 3C 273 due to unreasonably high magnetic field and jet power values. However, several HSP BL Lacs were fit with a similar hadronic model by Cerruti et al. [37], which gave more reasonable jet powers. Petropoulou & Mastichiadis [121] show that a signature of hadronic models of BL Lac objects is a bump at $\approx$ 40 keV to 40 MeV from synchrotron emission of pairs produced by the Bethe-Heitler process. Such a feature may be detectable by future γ-ray telescopes sensitive in this range. Aside from energetics, leptonic and hadronic models could be distinguished through the detection of a very-high energy neutrino by IceCube or another such detector coincident in direction and time with a γ-ray flare [51, 120], or through polarization of X-rays or γ-rays [143]. Several authors have recently developed time-dependent hadronic models [52, 51], which could offer an additional and probably more observationally realistic way to discriminate between leptonic and hadronic models.

If blazars are the source of UHECRs, then it is possible that cosmic rays that escape the blazar itself could make an observational signature through pion production and decay through pγ interactions with the EBL and CMB. This could explain the non-variable VHE emission for HSP BL Lacs [60, 59, 58].

7. Acknowledgments

I am grateful to Soebur Razzaque for the invitation to visit the University of Johannesburg and

to attend and speak at the HEASA meeting, and to Andrew Chen for the opportunity to visit the University of Witwatersrand. I am also grateful to Markus Böttcher for the additional opportunity to visit his group in Potchefstroom. Charles Dermer, Teddy Cheung, and Anna Barnacka have my thanks for proofreading portions of this manuscript (any mistakes are soley my responsibility). Some of my research presented here was funded by the Chief of Naval Research and by NASA *Fermi* Guest Investigator grants.

References

[1] A. A. Abdo, M. Ackermann, M. Ajello, et al., *Bright Active Galactic Nuclei Source List from the First Three Months of the Fermi Large Area Telescope All-Sky Survey*, ApJ, 700 (2009), pp. 597–622.

[2] ———, *Early Fermi Gamma-ray Space Telescope Observations of the Quasar 3C 454.3*, ApJ, 699 (2009), pp. 817–823.

[3] ———, *Fermi Large Area Telescope View of the Core of the Radio Galaxy Centaurus A*, ApJ, 719 (2010), pp. 1433–1444.

[4] ———, *Spectral Properties of Bright Fermi-Detected Blazars in the Gamma-Ray Band*, ApJ, 710 (2010), pp. 1271–1285.

[5] ———, *The First Catalog of Active Galactic Nuclei Detected by the Fermi Large Area Telescope*, ApJ, 715 (2010), pp. 429–457.

[6] ———, *The Spectral Energy Distribution of Fermi Bright Blazars*, ApJ, 716 (2010), pp. 30–70.

[7] ———, *Fermi Gamma-ray Space Telescope Observations of the Gamma-ray Outburst from 3C454.3 in November 2010*, ApJL, 733 (2011), p. L26.

[8] ———, *Fermi Large Area Telescope Observations of Markarian 421: The Missing Piece of its Spectral Energy Distribution*, ApJ, 736 (2011), p. 131.

[9] ———, *Gamma-Ray Flaring Activity from the Gravitationally Lensed Blazar PKS 1830–211 Observed by Fermi LAT*, ApJ, 799 (2015), p. 143.

[10] A. Abramowski, F. Acero, F. Aharonian, et al., *H.E.S.S. discovery of VHE γ-rays from the quasar PKS 1510-089*, A&A, 554 (2013), p. A107.

[11] F. Acero, M. Ackermann, M. Ajello, et al., *Fermi Large Area Telescope Third Source Catalog*, ApJS, 218 (2015), p. 23.

[12] M. Ackermann, M. Ajello, A. Allafort, et al., *Multifrequency Studies of the Peculiar Quasar 4C +21.35 during the 2010 Flaring Activity*, ApJ, 786 (2014), p. 157.

[13] M. Ackermann, M. Ajello, W. Atwood, et al., *The Second Catalog of Active Galactic Nuclei Detected by the Fermi Large Area Telescope*, ApJ, 743 (2011), p. 171.

[14] ———, *The Third Catalog of Active Galactic Nuclei Detected by the Fermi Large Area Telescope*, arXiv:1501.06054, (2015).

[15] M. Ackermann, M. Ajello, L. Baldini, et al., *Fermi Gamma-ray Space Telescope Observations of Gamma-ray Outbursts from 3C 454.3 in 2009 December and 2010 April*, ApJ, 721 (2010), pp. 1383–1396.

[16] I. Agudo, A. P. Marscher, S. G. Jorstad, et al., *On the Location of the γ-Ray Outburst Emission in the BL Lacertae Object AO 0235+164 Through Observations Across the Electromagnetic Spectrum*, ApJL, 735 (2011), p. L10.

[17] F. Aharonian, A. G. Akhperjanian, G. Anton, et al., *Simultaneous multiwavelength observations of the second exceptional γ-ray flare of PKS 2155-304 in July 2006*, A&A, 502 (2009), pp. 749–770.

[18] M. Ajello, R. W. Romani, D. Gasparrini, et al., *The Cosmic Evolution of Fermi BL Lacertae Objects*, ApJ, 780 (2014), p. 73.

[19] M. Ajello, M. S. Shaw, R. W. Romani, et al., *The Luminosity Function of Fermi-detected Flat-spectrum Radio Quasars*, ApJ, 751 (2012), p. 108.

[20] J. Albert et al., *Very-High-Energy gamma rays from a Distant Quasar: How Transparent Is the Universe?*, Science, 320 (2008), pp. 1752–.

[21] J. Aleksić, S. Ansoldi, L. A. Antonelli, et al., *MAGIC gamma-ray and multi-frequency observations of flat spectrum radio quasar PKS 1510-089 in early 2012*, A&A, 569 (2014), p. A46.

[22] J. Aleksić, L. A. Antonelli, P. Antoranz, et al., *MAGIC Discovery of Very High Energy Emission from the FSRQ PKS 1222+21*, ApJL, 730 (2011), p. L8.

[23] W. B. Atwood, A. A. Abdo, M. Ackermann, et al., *The Large Area Telescope on the Fermi Gamma-Ray Space Telescope Mission*, ApJ, 697 (2009), pp. 1071–1102.

[24] A. Barnacka, M. J. Geller, I. P. Dell'Antonio, and W. Benbow, *Strong Gravitational Lensing as a Tool to Investigate the Structure of Jets at High Energies*, ApJ, 788 (2014), p. 139.

[25] ———, *Resolving the High-energy Universe with Strong Gravitational Lensing: The Case of PKS 1830−211*, ApJ, 809 (2015), p. 100.

[26] A. Barnacka, J.-F. Glicenstein, and Y. Moudden, *First evidence of a gravitational lensing-induced echo in gamma rays with Fermi LAT*, A&A, 528 (2011), p. L3.

[27] M. C. Bentz, K. D. Denney, C. J. Grier, et al., *The Low-luminosity End of the Radius-Luminosity Relationship for Active Galactic Nuclei*, ApJ, 767 (2013), p. 149.

[28] M. C. Bentz, B. M. Peterson, R. W. Pogge, M. Vestergaard, and C. A. Onken, *The Radius-Luminosity Relationship for Active Galactic Nuclei: The Effect of Host-Galaxy Starlight on Luminosity Measurements*, ApJ, 644 (2006), pp. 133–142.

[29] E. W. Bonning, C. Bailyn, C. M. Urry, M. Buxton, G. Fossati, L. Maraschi, P. Coppi, R. Scalzo, J. Isler, and A. Kaptur, *Correlated Variability in the Blazar 3C 454.3*, ApJL, 697 (2009), pp. L81–L85.

[30] M. Böttcher and C. D. Dermer, *An Evolutionary Scenario for Blazar Unification*, ApJ, 564 (2002), pp. 86–91.

[31] M. Böttcher and D. Principe, *Optical Variability of the Quasar 3C 279: The Signature of a Decelerating Jet?*, ApJ, 692 (2009), pp. 1374–1381.

[32] M. Böttcher, A. Reimer, K. Sweeney, and A. Prakash, *Leptonic and Hadronic Modeling of Fermi-detected Blazars*, ApJ, 768 (2013), p. 54.

[33] A. M. Brown, *Locating the γ-ray emission region of the flat spectrum radio quasar PKS 1510-089*, MNRAS, 431 (2013), pp. 824–835.

[34] S. Buson, F. Longo, S. Larsson, et al., *Unusual flaring activity in the blazar PKS 1424-418 during 2008-2011*, A&A, 569 (2014), p. A40.

[35] A. Cavaliere and V. D'Elia, *The Blazar Main Sequence*, ApJ, 571 (2002), pp. 226–233.

[36] M. Cerruti, C. D. Dermer, B. Lott, C. Boisson, and A. Zech, *Gamma-Ray Blazars near Equipartition and the Origin of the GeV Spectral Break in 3C 454.3*, ApJL, 771 (2013), p. L4.

[37] M. Cerruti, A. Zech, C. Boisson, and S. Inoue, *A hadronic origin for ultra-high-frequency-peaked BL Lac objects*, MNRAS, 448 (2015), pp. 910–927.

[38] R. Chatterjee, C. D. Bailyn, E. W. Bonning, M. Buxton, P. Coppi, G. Fossati, J. Isler, L. Maraschi, and C. M. Urry, *Similarity of the Optical-Infrared and γ-Ray Time Variability of Fermi Blazars*, ApJ, 749 (2012), p. 191.

[39] R. Chatterjee, G. Fossati, C. M. Urry, C. D. Bailyn, L. Maraschi, M. Buxton, E. W. Bonning, J. Isler, and P. Coppi, *An Optical-Near-infrared Outburst with no Accompanying γ-Rays in the Blazar PKS 0208-512*, ApJL, 763 (2013), p. L11.

[40] L. Chen and J. M. Bai, *Implications for the Blazar Sequence and Inverse Compton Models from Fermi Bright Blazars*, ApJ, 735 (2011), pp. 108–+.

[41] C. C. Cheung, S. Larsson, J. D. Scargle, et al., *Fermi Large Area Telescope Detection of Gravitational Lens Delayed γ-Ray Flares from Blazar B0218+357*, ApJL, 782 (2014), p. L14.

[42] M. Chiaberge, A. Capetti, and A. Celotti, *The BL Lac heart of Centaurus A*, MNRAS, 324 (2001), pp. L33–L37.

[43] M. Chiaberge, A. Celotti, A. Capetti, and G. Ghisellini, *Does the unification of BL Lac and FR I radio galaxies require jet velocity structures?*, A&A, 358 (2000), pp. 104–112.

[44] D. P. Cohen, R. W. Romani, A. V. Filippenko, S. B. Cenko, B. Lott, W. Zheng, and W. Li, *Temporal Correlations between Optical and Gamma-Ray Activity in Blazars*, ApJ, 797 (2014), p. 137.

[45] F. D'Ammando, E. Antolini, G. Tosti, et al., *Long-term monitoring of PKS 0537-441 with Fermi-LAT and multiwavelength observations*, MNRAS, 431 (2013), pp. 2481–2492.

[46] C. D. Dermer, K. Murase, and H. Takami, *Variable Gamma-Ray Emission Induced by Ultra-high Energy Neutral Beams: Application to 4C +21.35*, ApJ, 755 (2012), p. 147.

[47] C. D. Dermer and S. Razzaque, *Acceleration of Ultra-high-energy Cosmic Rays in the Colliding Shells of Blazars and Gamma-ray Bursts: Constraints from the Fermi Gamma-ray Space Telescope*, ApJ, 724 (2010), pp. 1366–1372.

[48] C. D. Dermer and R. Schlickeiser, *Model for the High-Energy Emission from Blazars*, ApJ, 416 (1993), pp. 458–+.

[49] ——, *Transformation Properties of External Radiation Fields, Energy-Loss Rates and Scattered Spectra, and a Model for Blazar Variability*, ApJ, 575 (2002), pp. 667–686.

[50] C. D. Dermer, D. Yan, L. Zhang, J. D. Finke, and B. Lott, *Near-Equipartition Jets with Log-Parabola Electron Energy Distribution and the Blazar Spectral-Index Diagrams*, arXiv:1504.03228, (2015).

[51] C. Diltz, M. Böttcher, and G. Fossati, *Time Dependent Hadronic Modeling of Flat Spectrum Radio Quasars*, ApJ, 802 (2015), p. 133.

[52] S. Dimitrakoudis, A. Mastichiadis, R. J. Protheroe, and A. Reimer, *The time-dependent one-zone hadronic model. First principles*, A&A, 546 (2012), p. A120.

[53] L. Dondi and G. Ghisellini, *Gamma-ray-loud blazars and beaming*, MNRAS, 273 (1995), pp. 583–595.

[54] Dotson, A., Georganopoulos, M., Meyer, E. T., & McCann, K. *On the Location of the 2009 GeV Flares of Blazar PKS 1510-089* ApJ, 809, (2015), p. 164

[55] A. Dotson, M. Georganopoulos, D. Kazanas, and E. S. Perlman, *A Method for Localizing Energy Dissipation in Blazars Using Fermi Variability*, ApJL, 758 (2012), p. L15.

[56] M. S. Dutka, R. Ojha, K. Pottschmidt, et al., *Multi-wavelength Observations of PKS 2142-75 during Active and Quiescent Gamma-Ray States*, ApJ, 779 (2013), p. 174.

[57] M. Elvis, D. Plummer, J. Schachter, and G. Fabbiano, *The Einstein Slew Survey*, ApJS, 80 (1992), pp. 257–303.

[58] W. Essey, O. Kalashev, A. Kusenko, and J. F. Beacom, *Role of Line-of-sight Cosmic-ray Interactions in Forming the Spectra of Distant Blazars in TeV Gamma Rays and High-energy Neutrinos*, ApJ, 731 (2011), p. 51.

[59] W. Essey, O. E. Kalashev, A. Kusenko, and J. F. Beacom, *Secondary Photons and Neutrinos from Cosmic Rays Produced by Distant Blazars*, Physical Review Letters, 104 (2010), p. 141102.

[60] W. Essey and A. Kusenko, *A new interpretation of the gamma-ray observations of distant active galactic nuclei*, Astroparticle Physics, 33 (2010), pp. 81–85.

[61] B. L. Fanaroff and J. M. Riley, *The morphology of extragalactic radio sources of high and low luminosity*, MNRAS, 167 (1974), pp. 31P–36P.

[62] J. Finke, *Blazars in Context in the Fermi Era*, arXiv:1303.5095, (2013).

[63] J. D. Finke, *Compton Dominance and the Blazar Sequence*, ApJ, 763 (2013), p. 134.

[64] J. D. Finke and P. A. Becker, *Fourier Analysis of Blazar Variability*, ApJ, 791 (2014), p. 21.

[65] ——, *Fourier Analysis of Blazar Variability: Klein-Nishina Effects and the Jet Scattering Environment*, ApJ, 809 (2015), p. 85.

[66] J. D. Finke and C. D. Dermer, *On the Break in the Fermi-Large Area Telescope Spectrum of 3C 454.3*, ApJL, 714 (2010), pp. L303–L307.

[67] G. Fossati et al., *Multiwavelength Observations of Markarian 421 in 2001 March: An Unprecedented View on the X-Ray/TeV Correlated Variability*, ApJ, 677 (2008), pp. 906–925.

[68] G. Fossati, L. Maraschi, A. Celotti, A. Comastri, and G. Ghisellini, *A unifying view of the spectral energy distributions of blazars*, MNRAS, 299 (1998), pp. 433–448.

[69] Y. Fukazawa, J. Finke, Ł. Stawarz, Y. Tanaka, R. Itoh, and S. Tokuda, *Suzaku Observations of γ-Ray Bright Radio Galaxies: Origin of the X-Ray Emission and Broadband Modeling*, ApJ, 798 (2015), p. 74.

[70] G. Ghisellini, A. Celotti, G. Fossati, L. Maraschi, and A. Comastri, *A theoretical unifying scheme for gamma-ray bright blazars*, MNRAS, 301 (1998), pp. 451–468.

[71] G. Ghisellini, F. Tavecchio, and M. Chiaberge, *Structured jets in TeV BL Lac objects and radiogalaxies. Implications for the observed properties*, A&A, 432 (2005), pp. 401–410.

[72] G. Ghisellini, F. Tavecchio, L. Foschini, G. Bonnoli, and G. Tagliaferri, *The red blazar PMN J2345-1555 becomes blue*, MNRAS, 432 (2013), p. L66.

[73] G. Ghisellini, F. Tavecchio, L. Foschini, and G. Ghirlanda, *The transition between BL Lac objects and flat spectrum radio quasars*, MNRAS, 414 (2011), pp. 2674–2689.

[74] G. Ghisellini, F. Tavecchio, L. Foschini, T. Sbarrato, G. Ghirlanda, and L. Maraschi, *Blue Fermi flat spectrum radio quasars*, MNRAS, 425 (2012), pp. 1371–1379.

[75] P. Giommi, P. Padovani, M. Perri, H. Landt, and E. Perlman, *Parameter Correlations and Cosmological Properties of BL Lac Objects*, in Blazar Astrophysics with BeppoSAX and Other Observatories, P. Giommi, E. Massaro, & G. Palumbo, ed., 2002, pp. 133–+.

[76] P. Giommi, P. Padovani, G. Polenta, S. Turriziani, V. D'Elia, and S. Piranomonte, *A simplified view of blazars: clearing the fog around long-standing selection effects*, MNRAS, 420 (2012), pp. 2899–2911.

[77] P. Giommi, S. Piranomonte, M. Perri, and P. Padovani, *The sedentary survey of extreme high energy peaked BL Lacs*, A&A, 434 (2005), pp. 385–396.

[78] P. Grandi, E. Torresi, and on behalf of the FERMI-LAT collaboration, *Exploring the FRI/FRII radio dichotomy with the Fermi satellite*, ArXiv:1205.1686, (2012).

[79] J. Harris, M. K. Daniel, and P. M. Chadwick, *Identifying Breaks and Curvature in the Fermi Spectra of Bright Flat Spectrum Radio Quasars*, ApJ, 761 (2012), p. 2.

[80] T. W. Jones, S. L. O'dell, and W. A. Stein, *Physics of Compact Nonthermal Sources. I. Theory of Radiation Processes*, ApJ, 188 (1974), pp. 353–368.

[81] ———, *Physics of Compact Nonthermal Sources. II. Determination of Physical Parameters*, ApJ, 192 (1974), pp. 261–278.

[82] S. G. Jorstad et al., *Polarimetric Observations of 15 Active Galactic Nuclei at High Frequencies: Jet Kinematics from Bimonthly Monitoring with the Very Long Baseline Array*, AJ, 130 (2005), pp. 1418–1465.

[83] S. G. Jorstad, A. P. Marscher, J. R. Mattox, M. F. Aller, H. D. Aller, A. E. Wehrle, and S. D. Bloom, *Multiepoch Very Long Baseline Array Observations of EGRET-detected Quasars and BL Lacertae Objects: Connection between Superluminal Ejections and Gamma-Ray Flares in Blazars*, ApJ, 556 (2001), pp. 738–748.

[84] J. Kataoka, J. R. Mattox, J. Quinn, H. Kubo, F. Makino, T. Takahashi, S. Inoue, R. C. Hartman, G. M. Madejski, P. Sreekumar, and S. J. Wagner, *High-Energy Emission from the TEV Blazar Markarian 501 during Multiwavelength Observations in 1996*, ApJ, 514 (1999), pp. 138–147.

[85] Kauffmann, G., Heckman, T. M., Tremonti, C., et al., *The host galaxies of active galactic nuclei*, MNRAS, 346, (2003), pp. 1055-1077.

[86] Kellermann, K. I., Sramek, R., Schmidt, M., Shaffer, D. B., & Green, R., *VLA observations of objects in the Palomar Bright Quasar Survey* AJ, 98, (1989), pp. 1195-1207

[87] A. Konigl, *Relativistic jets as X-ray and gamma-ray sources*, ApJ, 243 (1981), pp. 700–709.

[88] H. Kuehr, A. Witzel, I. I. K. Pauliny-Toth, and U. Nauber, *A catalogue of extragalactic radio sources having flux densities greater than 1 Jy at 5 GHz*, A&AS, 45 (1981), pp. 367–430.

[89] A. Lähteenmäki and E. Valtaoja, *Testing of Inverse Compton Models for Active Galactic Nuclei with Gamma-Ray and Radio Observations*, ApJ, 590 (2003), pp. 95–108.

[90] H. Landt and H. E. Bignall, *On the relationship between BL Lacertae objects and radio galaxies*, MNRAS, 391 (2008), pp. 967–985.

[91] H. Landt, P. Padovani, E. S. Perlman, and P. Giommi, *A physical classification scheme for blazars*, MNRAS, 351 (2004), pp. 83–100.

[92] J. León-Tavares, E. Valtaoja, M. Tornikoski, A. Lähteenmäki, and E. Nieppola, *The connection between gamma-ray emission and millimeter flares in Fermi/LAT blazars*, A&A, 532 (2011), p. A146.

[93] M. L. Lister, M. H. Cohen, D. C. Homan, M. Kadler, K. I. Kellermann, Y. Y. Kovalev, E. Ros, T. Savolainen, and J. A. Zensus, *MOJAVE: Monitoring of Jets in Active Galactic Nuclei with VLBA Experiments. VI. Kinematics Analysis of a Complete Sample of Blazar Jets*, AJ, 138 (2009), pp. 1874–1892.

[94] N. R. MacDonald, A. P. Marscher, S. G. Jorstad, and M. Joshi, *Through the Ring of Fire: Gamma-Ray Variability in Blazars by a Moving Plasmoid Passing a Local Source of Seed Photons*, ApJ, 804 (2015), p. 111.

[95] K. Mannheim, *The proton blazar*, A&A, 269 (1993), pp. 67–76.

[96] K. Mannheim and P. L. Biermann, *Gamma-ray flaring of 3C 279 - A proton-initiated cascade in the jet?*, A&A, 253 (1992), pp. L21–L24.

[97] M. J. M. Marcha, I. W. A. Browne, C. D. Impey, and P. S. Smith, *Optical spectroscopy and polarization of a new sample of optically bright flat radio spectrum sources*, MNRAS, 281 (1996), pp. 425–448.

[98] A. P. Marscher, *Turbulent, Extreme Multi-zone Model for Simulating Flux and Polarization Variability in Blazars*, ApJ, 780 (2014), p. 87.

[99] A. P. Marscher et al., *The inner jet of an active galactic nucleus as revealed by a radio-to-γ-ray outburst*, Nature, 452 (2008), pp. 966–969.

[100] ——, *Probing the Inner Jet of the Quasar PKS 1510-089 with Multi-Waveband Monitoring During Strong Gamma-Ray Activity*, ApJL, 710 (2010), pp. L126–L131.

[101] A. P. Marscher, S. G. Jorstad, I. Agudo, N. R. MacDonald, and T. L. Scott, *Relation between Events in the Millimeter-wave Core and Gamma-ray Outbursts in Blazar Jets*, arXiv:1204.6707, (2012).

[102] O. Mena and S. Razzaque, *Hints of an axion-like particle mixing in the GeV gamma-ray blazar data?*, JCAP, 11 (2013), p. 23.

[103] E. T. Meyer, G. Fossati, M. Georganopoulos, and M. L. Lister, *From the Blazar Sequence to the Blazar Envelope: Revisiting the Relativistic Jet Dichotomy in Radio-loud Active Galactic Nuclei*, ApJ, 740 (2011), pp. 98–+.

[104] ——, *Collective Evidence for Inverse Compton Emission from External Photons in High-power Blazars*, ApJL, 752 (2012), p. L4.

[105] R. Mirzoyan, *Discovery of Very High Energy Gamma-Ray Emission From Gravitationally Lensed Blazar S3 0218+357 With the MAGIC Telescopes*, The Astronomer's Telegram, 6349 (2014), p. 1.

[106] ——, *Discovery of Very High Energy Gamma-Ray Emission from the distant FSRQ PKS 1441+25 with the MAGIC telescopes*, The Astronomer's Telegram, 7416 (2015), p. 1.

[107] A. Mücke and R. J. Protheroe, *A proton synchrotron blazar model for flaring in Markarian 501*, Astroparticle Physics, 15 (2001), pp. 121–136.

[108] A. Mücke, R. J. Protheroe, R. Engel, J. P. Rachen, and T. Stanev, *BL Lac objects in the synchrotron proton blazar model*, Astroparticle Physics, 18 (2003), pp. 593–613.

[109] R. Mukherjee, *Very-high-energy gamma-ray emission from PKS 1441+25 detected with VERITAS*, The Astronomer's Telegram, 7433 (2015), p. 1.

[110] K. Nakagawa and M. Mori, *Time Series Analysis of Gamma-Ray Blazars and Implications for the Central Black-hole Mass*, ApJ, 773 (2013), p. 177.

[111] K. Nalewajko, M. C. Begelman, and M. Sikora, *Constraining the Location of Gamma-Ray Flares in Luminous Blazars*, ApJ, 789 (2014), p. 161.

[112] M. Nenkova, M. M. Sirocky, Ž. Ivezić, and M. Elitzur, *AGN Dusty Tori. I. Handling of Clumpy Media*, ApJ, 685 (2008), pp. 147–159.

[113] M. Nenkova, M. M. Sirocky, R. Nikutta, Ž. Ivezić, and M. Elitzur, *AGN Dusty Tori. II. Observational Implications of Clumpiness*, ApJ, 685 (2008), pp. 160–180.

[114] A. Neronov, I. Vovk, and D. Malyshev, *Central engine of a gamma-ray blazar resolved through the magnifying glass of gravitational microlensing*, Nature Physics, 11 (2015), pp. 664–667.

[115] E. Nieppola, M. Tornikoski, and E. Valtaoja, *Spectral energy distributions of a large sample of BL Lacertae objects*, A&A, 445 (2006), pp. 441–450.

[116] L. Pacciani, F. Tavecchio, I. Donnarumma, A. Stamerra, L. Carrasco, E. Recillas, A. Porras, and M. Uemura, *Exploring the Blazar Zone in High-energy Flares of FSRQs*, ApJ, 790 (2014), p. 45.

[117] P. Padovani, P. Giommi, and A. Rau, *The discovery of high-power high synchrotron peak blazars*, MNRAS, 422 (2012), p. L48.

[118] P. Padovani, E. S. Perlman, H. Landt, P. Giommi, and M. Perri, *What Types of Jets Does Nature Make? A New Population of Radio Quasars*, ApJ, 588 (2003), pp. 128–142.

[119] M. Petropoulou and S. Dimitrakoudis, *Constraints of flat spectrum radio quasars in the hadronic model: the case of 3C 273*, MNRAS, 452 (2015), pp. 1303–1315.

[120] M. Petropoulou, S. Dimitrakoudis, P. Padovani, A. Mastichiadis, and E. Resconi, *Photohadronic origin of γ -ray BL Lac emission: implications for IceCube neutrinos*, MNRAS, 448 (2015), pp. 2412–2429.

[121] M. Petropoulou and A. Mastichiadis, *Bethe-Heitler emission in BL Lacs: filling the gap between X-rays and γ-rays*, MNRAS, 447 (2015), pp. 36–48.

[122] J. Poutanen and B. Stern, *GeV Breaks in Blazars as a Result of Gamma-ray Absorption Within the Broad-line Region*, ApJL, 717 (2010), pp. L118–L121.

[123] V. Ramakrishnan, T. Hovatta, E. Nieppola, M. Tornikoski, A. Lähteenmäki, and E. Valtaoja, *Locating the γ-ray emission site in Fermi/LAT blazars from correlation analysis between 37 GHz radio and γ-ray light curves*, MNRAS, 452 (2015), pp. 1280–1294.

[124] B. Rani, T. P. Krichbaum, L. Fuhrmann, et al., *Radio to gamma-ray variability study of blazar S5 0716+714*, A&A, 552 (2013), p. A11.

[125] A. Rau, P. Schady, J. Greiner, et al., *BL Lacertae objects beyond redshift 1.3 - UV-to-NIR photometry and photometric redshift for Fermi/LAT blazars*, A&A, 538 (2012), p. A26.

[126] A. Reimer, *The Redshift Dependence of Gamma-Ray Absorption in the Environments of Strong-Line AGNs*, ApJ, 665 (2007), pp. 1023–1029.

[127] A. Ringwald, *Exploring the role of axions and other WISPs in the dark universe*, Physics of the Dark Universe, 1 (2012), pp. 116–135.

[128] S. Saito, L. Stawarz, Y. Tanaka, T. Takahashi, M. Sikora, and R. Moderski, *Time-Dependent Modeling of Gamma-ray Flares in Blazar PKS1510-089*, arXiv:1507.02442, (2015).

[129] S. Saito, Ł. Stawarz, Y. T. Tanaka, T. Takahashi, G. Madejski, and F. D'Ammando, *Very Rapid High-amplitude Gamma-Ray Variability in Luminous Blazar PKS 1510-089 Studied with Fermi-LAT*, ApJL, 766 (2013), p. L11.

[130] M. Sikora, M. C. Begelman, and M. J. Rees, *Comptonization of diffuse ambient radiation by a relativistic jet: The source of gamma rays from blazars?*, ApJ, 421 (1994), pp. 153–162.

[131] M. A. Sobolewska, A. Siemiginowska, B. C. Kelly, and K. Nalewajko, *Stochastic Modeling of the Fermi/LAT γ-Ray Blazar Variability*, ApJ, 786 (2014), p. 143.

[132] B. E. Stern and J. Poutanen, *The Mystery of Spectral Breaks: Lyman Continuum Absorption by Photon-Photon Pair Production in the Fermi GeV Spectra of Bright Blazars*, ApJ, 794 (2014), p. 8.

[133] J. T. Stocke, S. L. Morris, I. M. Gioia, T. Maccacaro, R. Schild, A. Wolter, T. A. Fleming, and J. P. Henry, *The Einstein Observatory Extended Medium-Sensitivity Survey. II - The optical identifications*, ApJS, 76 (1991), pp. 813–874.

[134] F. Tavecchio, G. Ghisellini, G. Bonnoli, and G. Ghirlanda, *Constraining the location of the emitting region in Fermi blazars through rapid γ-ray variability*, MNRAS, 405 (2010), pp. L94–L98.

[135] F. Tavecchio, L. Maraschi, and G. Ghisellini, *Constraints on the Physical Parameters of TeV Blazars*, ApJ, 509 (1998), pp. 608–619.

[136] F. Tavecchio, M. Roncadelli, G. Galanti, and G. Bonnoli, *Evidence for an axion-like particle from PKS 1222+216?*, Phys. Rev. D, 86 (2012), p. 085036.

[137] G. Tosti, J. Chiang, B. Lott, E. Do Couto E Silva, J. E. Grove, and J. G. Thayer, *GLAST-LAT detection of extraordinary gamma-ray activity in 3C 454.3*, The Astronomer's Telegram, 1628 (2008), pp. 1–+.

[138] C. M. Urry and P. Padovani, *Unified Schemes for Radio-Loud Active Galactic Nuclei*, PASP, 107 (1995), pp. 803–+.

[139] I. Vovk and A. Neronov, *Microlensing constraint on the size of the gamma-ray emission region in blazar B0218+357*, ArXiv e-prints, (2015).

[140] J. V. Wall and J. A. Peacock, *Bright extragalactic radio sources at 2.7 GHz. III - The all-sky catalogue*, MNRAS, 216 (1985), pp. 173–192.

[141] M. Zacharias and R. Schlickeiser, *A new ordering parameter of spectral energy distributions from synchrotron self-Compton emitting blazars*, MNRAS, 420 (2012), pp. 84–102.

[142] A. A. Zdziarski and M. Böttcher, *Hadronic models of blazars require a change of the accretion paradigm*, MNRAS, 450 (2015), pp. L21–L25.

[143] H. Zhang and M. Böttcher, *X-Ray and Gamma-Ray Polarization in Leptonic and Hadronic Jet Models of Blazars*, ApJ, 774 (2013), p. 18.

[144] H. Zhang, X. Chen, M. Böttcher, F. Guo, and H. Li, *Polarization Swings Reveal Magnetic Energy Dissipation in Blazars*, ApJ, 804 (2015), p. 58.